energies

MDPI

Article

Optimal Management of Commercial Electric Vehicle Fleets with Recharging Stations and Time-Varying Electricity Prices

Massimiliano Coppo [1,*], Marco Agostini [1], Giulia De Matteis [2] and Marina Bertolini [3]

[1] Department of Industrial Engineering, University of Padova, 35131 Padova, Italy; marco.agostini.5@phd.unipd.it
[2] Department of Economics and Management "Marco Fanno", University of Padova, 35123 Padova, Italy; giulia.dematteis@studenti.unipd.it
[3] Department of Statistical Sciences, University of Padova, 35122 Padova, Italy; marina.bertolini@unipd.it
* Correspondence: massimiliano.coppo@unipd.it

Abstract: The promotion of electric mobility is a key objective of energy transition, and it is aimed at significantly reducing greenhouse gas emissions, with road transport being understood as a major contributor. Despite its potential, the adoption of electric vehicles (EVs) in logistics faces critical challenges, including limited battery range, charging time, and the availability of charging infrastructure. Moreover, deploying charging stations must be carefully coordinated with the public grid to ensure seamless integration. This paper proposes a novel methodology for the optimal design and management of EV fleets in logistics. Our approach introduces innovations such as leveraging self-produced electricity and incorporating time-varying energy prices that can be tailored to individual nodes. This marks an important step toward a comprehensive interdisciplinary framework that integrates technical solutions with public policy considerations. Through case studies, we explore how various parameters and resource distributions influence optimal decisions. The findings demonstrate significant potential for cost reduction and enhanced efficiency when applying this methodology to EV-based logistics, thereby offering actionable insights for advancing sustainable transportation.

Keywords: electric vehicles; logistics; vehicle routing problem; time-varying prices

Academic Editor: Chunhua Liu

Received: 3 December 2024
Revised: 13 January 2025
Accepted: 18 January 2025
Published: 21 January 2025

Citation: Coppo, M.; Agostini, M.; De Matteis, G.; Bertolini, M. Optimal Management of Commercial Electric Vehicle Fleets with Recharging Stations and Time-Varying Electricity Prices. *Energies* **2025**, *18*, 453. https://doi.org/10.3390/en18030453

1. Introduction

According to data in the IEA database, global CO_2 emissions related to the transport sector reached a value of 7.22 gigatons (Gt) in 2020 [1]. Specifically, when considering only road transport, the emission share was 5.66 Gt, which was about 18% of global energy-correlated CO_2 emissions in 2020 (31.5 Gt). According to the world energy outlook by IEA, the forecast scenarios foresee a continuous increase in the road transport emissions, reaching 5.89 (Gt) in 2030, which corresponds to an increase of 4% over 2020 [2].

The European Commission on 14 July 2021, presented the "Fit for 55" package, with the aim of achieving a reduction in European net greenhouse gas (GhG) emissions, taking 1990 as the base year. This reduction will be greater than, or equal to, 55% by 2030, eventually reaching 100% by mid-century. Such a resolution, among other climate goals, sets new caps to emissions from cars, enforcing a 55% decrease in emissions from the overall fleet compared to 2021, whereas a 50% reduction refers to light commercial vehicles. By 2035, new vehicles in the former two categories must be emission free.

Further back in time, the European Union had already adopted regulations specifically concerning vehicles and mobility for energy transition, such as Regulation (EU) 2019/631,

where the Union set the CO_2 emission reduction targets for new passenger cars and new light commercial vehicles, as well as mandated a 37.5% reduction in CO_2 emissions for new cars and 31% for new vans by 2030 when compared to the 2021 levels [3].

There are several works already ongoing to reduce the pollution caused by traditional engines [4], but electrification appears to be the most effective solution for operating. It can be seen how, concerning road transport, the electrification of vehicles has multiple benefits and is therefore the right direction to take in order to meet emission targets. Of course, electrification will be coupled with an increase in renewables and their integration, as also confirmed by the guidelines detailed in Directive (UE) 2018/2001 (RED II) [5]. According to the 2022 edition of the global electric vehicle outlook by IEA, a net reduction of 40 Mt CO_2-equivalent (eq) emitted indirectly was achieved in 2021 through the adoption of electric vehicles (EVs) [6]. According to IEA forecasts, the share of indirect emissions associated with the EV fleet is expected to be 340 Mt-CO_2-eq. If an equivalent fleet, but consisting of only internal combustion vehicles, were considered, the amount of GhG emitted would be 920 Mt-CO_2-eq. Therefore, EVs, in this forecast, would allow for a reduction of 580 Mt-CO_2-eq that would have otherwise gone into the atmosphere. A wider use of electric vehicles in urban logistics could translate to reduced noise pollution [7], thus opening new business opportunities like, for example, the possibility of increasing off-hour deliveries with multiple benefits in terms of emissions, traffic congestion, and road accidents [8,9].

Despite this evidence, the penetration of EVs is still limited, especially for commercial vehicles, due to barriers mixing technical issues and business behaviors [10,11]. The battery range, charging time, and availability are among the most critical issues [12] as they need a re-organization of transport activity [13]. More specifically, although commercial vehicles have a larger availability of space for hosting larger batteries, hence extending the range, this could reduce the total payload of the vehicle for commercial activity, thus potentially reducing the freight quantity in each trip [14]. Unlike conventional vehicles that can be refueled quickly, electric vehicles require longer charging periods, which can negatively affect operational efficiency and delivery times [15]. The need for planning alternative paths for EVs in order to take into account the limited range and the availability of recharging stations, as well as for reorganising shifts to accommodate charging times, is discussed in [11].

Under an economic perspective, externalities generated by transports not only refer to greenhouse gas emissions, but also other aspects such as traffic congestion, noise pollution, and road accidents, which all impose a cost on the collective [16,17] but may also, to some extent, represent (direct or indirect) costs for a logistic firm. On one hand, the internalization of external costs of transport has been put as a crucial objective for the EU strategy to promote sustainable mobility [18]; as such, logistics firms may soon be forced to incorporate the externalities generated in their cost function. On the other hand, some of these externalities already impact the operations both on the side of costs and lost profits. For example, traffic congestion and a lack of parking spots to upload/download goods can hamper deliveries, thus impacting the firm's profits and volumes, whereas damage to vehicles and goods due to road accidents may impose additional costs, along with human costs, to firms [19]. Road crashes impose costs on individuals (e.g., medical and human costs), firms (e.g., production losses and damage to property), as well as administrative costs [20]. In high-income countries, the share of these costs ranges from 0.5% to 6% of GDP, with human costs (i.e., all the immaterial costs of suffering, dying, and losing quality of life) representing the lion's share [20]. Though not being easily quantifiable, based on a survey with 8000 participants from four European countries (i.e., Belgium, France, Germany, and the Netherlands), the Value of a Statistical Life (VSL) lost due to road accidents is estimated in €6.2 million, more than six times the Value of a Statistical Serious Injury (VSSI), which

was evaluated in €950,000 [21]. Finally, the Value of Time (VoT) lost was estimated to be equal to €16 per hour.

When referring to the use of EVs specifically, the initial investment for purchasing the vehicles and for the installation of their charging infrastructure are among the main drawbacks [22]. However, considering the total cost for ownership (TCO), which includes purchase price, running costs, repairs, taxes, maintenance, depreciation, and resale value, Battery Electric Vehicles (BEVs) already present competitive values with respect to internal combustion engine vehicles (IECVs) [23]. The projection reported in Figure 1 shows a comparison of the main alternative fuels for commercial trucks, with BE showing the most potential in the short term, led mainly by lower fuel and maintenance costs. Regarding charging infrastructure investments, such facilities represent strategic assets to develop with the goal of improving the diffusion of electric mobility; hence. they should encompass a Public–Private Partnership (PPP). The role of PPP was investigated with reference to the application of special time-of-use tariffs to incentivize private owners to use public chargers in [24]. The experience of implementing PPP for combining electric vehicles charging and renewables in Mexico was presented in [25], showing how the synergy between those technologies could actually lead to a successful improvement in CO_2 emissions. Nonetheless, the literature that has focused on sustainable last mile logistics lacks economic contributions despite the topic presenting some typical themes of public finance, such as the generation of externalities and the need for collaboration between public and private sectors [26].

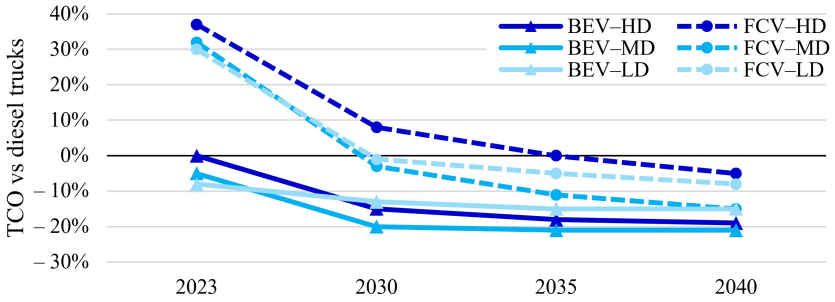

Figure 1. The expected trends for the TCO of Battery Electric Vehicles (BEVs) and Fuel Cell Vehicles (FCVs) in the main segments of trucks for freight transport (high-, medium-, and low-duty vehicles) with respect to IECVs [23].

Indeed, the potential for emission reductions from the electrification of commercial vehicles may be better exploited by implementing more specific policies, especially in urban contexts. Aside from the aforementioned policies aiming at forcing a progressive reduction of emissions in new vehicles, other measures could be designed to reduce the impact of freight transport in urban contexts. Some examples include restrictions to certain areas in specific periods [27,28], incentives for night deliveries [29,30], or dynamic tariffs for access to urban zones, which are differentiated depending on time and vehicle type [31,32]. Along with the traffic management policies, freight demand management should be accounted by regulation in order to improve the behavior of customers, such as, for example, by consolidating deliveries, as suggested in [33].

As a possible result of such policies, the electrification of freight transport could see a paradigm shift, leading to a "layered" operation, which is commonly referred to as a "multi-tier" or "multi-echelon" delivery system. A two-level distribution scheme was proposed to combine vans and electric cargo bikes in [34,35]. Such a paradigm would also open to a more rational use of the urban land, exploiting available areas by integrating multiple stakeholders in the planning and operation of logistics [36]. Other works proposed a multi-

service approach by combining passengers and freight transport to further rationalize the vehicle traffic in cities [37,38].

The development of optimal routing strategies has been appointed as an enabling feature in the process of increasing the penetration of EVs in commercial fleets. A comprehensive review of the current state of the art in electric vehicle routing problem (EVRP) applications was presented in [39], where a classification of approaches was proposed. Specific solutions to such problems in urban logistics were addressed in [40], while an approach based on battery swapping at recharging stations was proposed in [41].

Although the problem is well known and multiple solutions were proposed, there is a lack of studies that have specifically addressed the charging behavior expected for the vehicles' batteries during all periods. Methodologies for solving the electric vehicle routing problem by accounting for non-linear battery charging or different recharging technologies were proposed in [42–44] which, however, did not consider the time-varying prices of electricity. In [45,46], the authors proposed EVRP solutions to be applied to freight distribution and public transport problems, respectively, encompassing their interactions with time-varying prices, although not quite covering the entire daily period as the recharge was assumed as taking place after the end of delivery period with no regard to specific time intervals.

In addition to significantly reducing emissions, a broader adoption of EVs could enhance the resilience and sustainability of electrical systems, fostering the exploitation of renewable energy production. For instance, EV batteries can serve as effective storage solutions and be used for grid balancing purposes in what is commonly referred as vehicle-to-grid (V2G) technology, as vehicles are typically parked much of the time [47,48]. This storage potential can improve the allocation of renewable energy sources by helping to mitigate the timing mismatch between peak renewable energy production and peak demand [49]. In particular, electric distribution system operators can implement novel management schemes to face potential technical challenges in their networks by acquiring ancillary services for EVs, such as those possibly provided by storage-capable users [50–53].

The main scope of this work is to propose an optimal methodology to support the sizing and management of EVs for freight delivery. The methodology, using a mixed integer linear programming (MILP) approach, was designed to consider multiple time intervals within a given time horizon. With such a design, the adoption of time-varying energy prices is allowed, along with the exploitation of local production according to its availability. An analysis of different optimal decisions was conducted in relation to varying parameters on space, resource availability, and prices.

The features mentioned in the previous paragraph specifically represent the main novelty of the proposed approach with reference to literature that has treated the same kind of problem. Our approach introduces innovations, such as leveraging self-produced electricity and incorporating time-varying energy prices (which can be tailored to individual nodes). This marks an important step toward a comprehensive interdisciplinary framework that integrates technical solutions with public policy considerations.

The rest of this paper is organized as follows. Section 2 presents the methodology, with a focus on the main goal, the parameters, and the constraints. Section 3 presents the results with a case study and a parametric analysis to discuss the impact of different settings on optimal decisions. Section 4 draws the conclusions of this work.

2. Optimization Methodology

The optimization problem described in the following aims at minimizing the cost used for recharging the battery in the operation of a fleet of commercial electric vehicles

by taking into account a time-varying price for electricity that is either self-generated or purchased from the grid.

The objective function, as shown in (1), expresses the sum of the three cost items that are to be minimized:

$$min\left(C_v + C_{es} + C_{ep}\right), \tag{1}$$

where the cost items are defined as

$$C_v = \sum_{v \in V} \sum_{j \in S} \sum_{i \in N \setminus \{j\}} a_{i,j,0,v} \cdot c_{ev} \tag{2}$$

$$C_{es} = \sum_{v \in V} \sum_{g \in G} \sum_{i \in N} \sum_{k \in T} E'_{i,k,g,v} \cdot \pi_{s,i,k} \tag{3}$$

$$C_{ep} = \sum_{v \in V} \sum_{g \in G} \sum_{i \in N} \sum_{k \in T} E''_{i,k,g,v} \cdot \pi_{p,i,k}, \tag{4}$$

where the range of sum operators is indicated by the respective index reading elements in the relative set (e.g., $v \in V$ means for each vehicle v in set V).

As the number of vehicles required for the service is not known in advance, the adoption of a further vehicle increases cost C_v, as shown in (2), where c_{ev} represents the cost of owning a further vehicle for the considered time horizon.

The cost of energy to charge vehicles was divided into two cost items, C_{es} and C_{ep}, referring to the self-produced and purchased energy, respectively, as shown in (3) and (4). The former represents a cost for missed revenue on energy that is not sold when produced; hence, it is determined by totaling, for each vehicle v and each trip g, the amount of self-produced energy at each node i in each time interval k ($E'_{i,k,g,v}$) multiplied by the sale price $\pi_{s,i,k}$. A similar approach was used for defining the cost for energy purchase from the grid ($E''_{i,k,g,v}$), for which a purchase price $\pi_{p,i,k}$ was defined.

2.1. Parameters, Sets, and Variable Types

Some of the parameters used in the following constraints definition have to be assumed. Given the set of coordinates (x,y) for each node in the map, a set d of the distances of all of the nodes was created, as shown in (5). Then, two sets b and h were defined, containing, for each couple of nodes, the energy consumption and time required to perform the relative arc. As described in (6) and (7), the values in b and h were obtained by multiplying the distance in each arc by the average consumption γ_v in [kWh/km] and the average driving speed σ_v in [km/h], respectively, for each vehicle v. It should be noted that, in practice, these sets should result from a topographic analysis of the operation area to evaluate the specific energy consumption and required time depending on the slope, road conditions, traffic, and building density [54,55]. The model description, however, remains the same, as sets b and h could generically result from different unitary consumption and vehicle speed in each arc.

$$d_{i,j} = \sqrt{(x_i - x_j)^2 + (y_i - y_j)^2} \qquad (i,j) \in N, i \neq j \tag{5}$$

$$b_{i,j} = d_{i,j} \cdot \gamma_v \qquad v \in V,\ (i,j) \in N,\ i \neq j \tag{6}$$

$$h_{i,j} = d_{i,j} \cdot \sigma_v \qquad v \in V,\ (i,j) \in N,\ i \neq j \tag{7}$$

The characteristics of each vehicle v were defined through parameters related to the battery rated energy K_v and the minimum and maximum state of charge (SoC), $\underline{SOC}_v$, and $\overline{SOC}_v$, respectively, while the cargo capacity was limited by cap_v.

Energy recharge is allowed both at the depot and at nodes in which a recharging facility is located. In both cases, the recharging efficiency is assumed to be constant through

parameter η_c. The maximum recharge power and duration of the stop time for each node i and trip g are defined by parameters $p_{r,i,g}$ and $\tau_{i,g}$, respectively.

Map nodes indices are stored in set N, having subsets S, R, and D for depot node, nodes with recharging facilities, and pure delivery nodes, respectively. Further sets G and V are defined for available indices of trips and vehicles, respectively. Finally, a set T contains the time intervals considered in the time horizon.

Optimization variables are designed according to the three types, as depicted in Figure 2. The type in Figure 2a is used to store values concerning the arcs between couples of nodes (first two dimensions) in different trips (third dimension) and vehicles (fourth dimension). The type in Figure 2b is similar to the previous one, but having the second dimension reduced to one element (i.e., one value for each node), while the type in Figure 2c has the same structure, but with the second dimension concerning to time intervals.

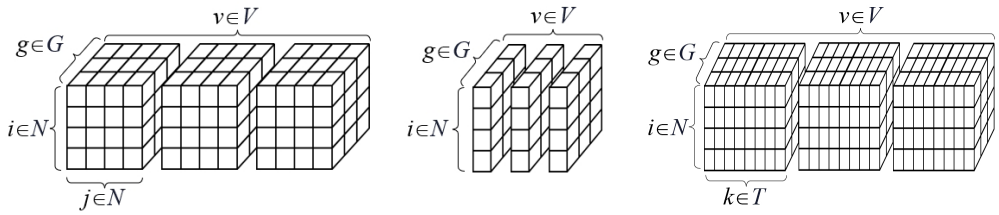

(**a**) (**b**) (**c**)

Figure 2. The variable types defined in the methodology: type (**a**) used for a, f, e, and t; type (**b**) used for E; and type (**c**) was used for w, E', and E''.

2.2. Vehicle Routing Problem Constraints

The set of equations in (8)–(14) define the constraints concerning routing of vehicles in the map nodes.

$$\sum_{v\in V}\sum_{g\in G}\sum_{j\in N\setminus\{i\}} a_{i,j,g,v} = 1 \qquad i\in D \tag{8}$$

$$\sum_{v\in V}\sum_{g\in G}\sum_{j\in N\setminus\{i\}} a_{j,i,g,v} = 1 \qquad i\in D \tag{9}$$

$$\sum_{v\in V}\sum_{g\in G}\sum_{j\in N\setminus\{i\}} a_{i,j,g,v} \geq 1 \qquad i\in R \tag{10}$$

$$\sum_{v\in V}\sum_{g\in G}\sum_{j\in N\setminus\{i\}} a_{j,i,g,v} \geq 1 \qquad i\in R \tag{11}$$

$$\sum_{j\in\setminus\{i\}} a_{j,i,g,v} \leq 1 \qquad v\in V,\ g=0,\ i\in S \tag{12}$$

$$\sum_{j\in\setminus\{i\}} a_{i,j,g,v} - \sum_{j\in\setminus\{i\}} a_{j,i,g,v} = 0 \qquad v\in V,\ g\in G,\ i\in N \tag{13}$$

$$\sum_{j\in\setminus\{i\}} a_{j,i,g,v} - \sum_{j\in\setminus\{i\}} a_{j,i,g-1,v} \leq 0 \qquad v\in V,\ g\in G\setminus\{0\},\ i\in S. \tag{14}$$

The binary optimization variable a, with the type shown in Figure 2a, is used to define the presence of a vehicle in a specific trip at a specific node. For example, $a_{i,j,g,v} = 1$, if vehicle v during trip g stops at bus i coming from bus j. The source node, which is stored in set S, indicates the depot from which all the vehicles began their trips and to which they had to return. Delivery nodes, which are stored in set D, have to be visited exactly once, as shown in (8) and (9), while the nodes with a recharge facility, which are stored in set R, may be visited more than once by one or more vehicles in different trips, as shown in (10) and (11).

The same is allowed for the depot, as a vehicle can return to it multiple times during operation. However, in such a case, a new trip is considered and stored in a separate layer

for all variables. A new vehicle may not be required but, when used, only one arc leaving and returning the depot was allowed, as shown in Equation (12).

Equations (13) and (14) ensure the arcs' continuity, with the former addressing the same layer in terms of vehicle and trip and the latter linking consecutive trips to ensure they are sequential.

2.3. Vehicle Transport Capacity Constraints

The constraints concerning the goods delivery at the map nodes are defined by the equations in (15) and (16).

$$\sum_{v\in V}\sum_{g\in G}\sum_{j\in N\setminus\{i\}} f_{i,j,g,v} - \sum_{v\in V}\sum_{g\in G}\sum_{j\in N\setminus\{i\}} f_{j,i,g,v} = q_i \qquad i\in D\cup R \tag{15}$$

$$0 \le f_{i,j,g,v} \le cap_v \cdot a_{i,j,g,v} \qquad v\in V,\ g\in G,\ i,j\in N, i\neq j \tag{16}$$

The continuous optimization variable f is defined by the type in Figure 2a and can be interpreted in the same way as a. It accounts for the freight volume stored in vehicle v during trip g while performing the generic arc i-j. All of the goods to be delivered were assumed to be homogeneous, such that they equally concur to the total freight volume quantity required at a delivery node (including those hosting a recharge facility), and they are stored in array q.

As shown in (15), the freight quantity in the vehicle is progressively reduced while moving between nodes i and j by the amount required at node i. Each vehicle could have a different freight volume capacity, expressed by parameter cap_v which defines the upper bound of variable f, as in (16).

2.4. Vehicle Energy Management Constraints

The management of energy usage and recharge is a key component of the developed methodology. The balance between the total energy added to the battery when recharging and the total consumption for each vehicle was forced by (17). Variable E was determined by the type shown in Figure 2b, and it was used to store the energy absorption by vehicle v during trip g at the respective node i.

$$\sum_{g\in G}\sum_{i\in N} E_{i,g,v}\cdot\eta_c - \sum_{g\in G}\sum_{j\in N}\sum_{i\in N\setminus\{j\}} b_{i,j}\cdot a_{i,j,g,v} = 0 \qquad v\in V. \tag{17}$$

Similarly to previous constraints, a four-dimensional continuous optimization variable e by the type shown in Figure 2a was defined to manage the energy stored in the vehicles at each stop in a grid node. The equations in (18)–(23) refer to constraints on such a variable for all the sets of grid nodes.

$$\sum_{j\in\setminus\{i\}} e_{i,j,g,v} - \sum_{j\in\setminus\{i\}} e_{j,i,g,v} - \sum_{j\in N\setminus\{i\}} b_{j,i}\cdot a_{j,i,g,v} + E_{i,g,v}\cdot\eta_c = 0 \quad v\in V,\ g\in G,\ i\in D\cup R \tag{18}$$

$$\sum_{j\in\setminus\{i\}} \left(e_{j,i,g,v} + b_{j,i}\cdot a_{j,i,g,v}\right) \le K_v\cdot\overline{SOC}_v \qquad v\in V,\ g\in G,\ i\in N \tag{19}$$

$$K_v\cdot\underline{SOC}_v\cdot a_{i,j,g,v} \le e_{i,j,g,v} \le K_v\cdot\overline{SOC}_v\cdot a_{i,j,g,v} \qquad v\in V,\ g\in G,\ i,j\in N, i\neq j \tag{20}$$

$$J_{i,g,v} = \sum_{k\in N\setminus\{i\}} e_{j,k,g-1,v} + E_{i,g,v}\cdot\eta_c - b_{i,j}\cdot a_{i,j,g,v} \qquad v\in V,\ g\in G\setminus\{0\},\ i\in N\setminus\{j\},\ j\in S \tag{21}$$

$$J_{i,g,v} - (1-a_{i,j,g,v})\cdot M \le e_{i,j,g,v} \le J_{i,g,v} \qquad v\in V,\ g\in G\setminus\{0\},\ i\in N\setminus\{j\},\ j\in S \tag{22}$$

$$0 \le e_{i,j,g,v} \le a_{i,j,g,v}\cdot M \qquad v\in V,\ g\in G\setminus\{0\},\ i\in N\setminus\{j\},\ j\in S. \tag{23}$$

As for (18), the amount of energy stored in vehicle v, in trip g, changes when moving between nodes i and j by the energy consumption in the movement, minus the energy absorbed at node i ($E_{i,g,v}$), multiplied by the charging efficiency η_c. Constraint (19) ensures

that the battery's residual energy at the receiving end of an arc (stored in e) plus the energy consumption along the arc itself do not exceed the battery's rated capacity. The values in e are bounded by the energy range of the battery in (20), and they are given by the product of rated energy K_v and the minimum and maximum SoC ($\underline{SOC}_v$ and $\overline{SOC}_v$). In the particular case of the depot node and for the trips after the first one, an auxiliary variable J was defined in (21). This was constrained through the *big-M* method in (22) and (23), with M an arbitrary large number, as in [56]. This approach was needed to keep the problem linear and to avoid non-convexity.

Specific constraints to the energy absorption by the vehicle were set by (24)–(27).

$$E_{i,g,v} = \sum_{k \in T} (E'_{i,k,g,v} + E''_{i,k,g,v}) \qquad v \in V,\ g \in G,\ i \in N \tag{24}$$

$$E_{i,g,v} \leq (1/\eta_c) \cdot \left(K_v \cdot \overline{SOC}_v - K_v \cdot \underline{SOC}_v\right) \cdot \sum_{j \in \setminus \{i\}} a_{j,i,g,v} \qquad v \in V,\ g \in G,\ i \in N \tag{25}$$

$$0 \leq E'_{i,k,g,v} \leq w_{i,k,g,v} \cdot p_{g,w} \cdot \min(\tau_{i,g}, 1) \qquad v \in V,\ k \in T,\ g \in G,\ i \in N \tag{26}$$

$$0 \leq E''_{i,k,g,v} \leq w_{i,k,g,v} \cdot p_{r,i,g} \cdot \min(\tau_{i,g}, 1) - E'_{i,k,g,v} \qquad v \in V,\ k \in T,\ g \in G,\ i \in N. \tag{27}$$

The amount of energy $E_{i,g,v}$ recharged in node i is the sum of the two components E' and E'', as in (24), thereby representing the share of the self-produced energy and the share of energy purchased from the grid in the entire time horizon, respectively. Energy $E_{i,g,v}$ is bounded in (25) by the vehicle's battery range, i.e., the range between maximum and minimum energy, which is divided by the charging efficiency η_c.

Concerning the self-production, in (26), E' is bounded between 0 and the product of the hourly average generated power and the stop time in each visiting window stored in array w, which is described in the following section. The stop time at each trip g and node i is defined by parameter $\tau_{i,g}$. Such a time can be less than one hour or multiple hours, depending on the type of service (e.g., delivery, fast-charging, or slow-charging); therefore, the share of exploitable self-production may be reduced if the stop time is less than one hour. The amount of energy purchased from the grid, E'', which is bounded in (27) between 0 and the available energy rechargeable (net of the self-production) depending on the maximum recharge power, is defined for each node and trip by parameter p_r, as well as the aforementioned stop time.

2.5. Time Constraints

As previously mentioned, a stop time was defined for each node, potentially different for each trip, through parameter $\tau_{i,g}$. Each vehicle is supposed to have a time limit for operation, and it is defined by parameter τ_{max}. Equation (28) defines variable z, and it was used in the following, referring to the total time required for each vehicle's overall travel, stops included, having removed the stop time before the beginning of service.

$$\sum_{g \in G} \sum_{j \in N} \sum_{i \in N \setminus \{j\}} \left(h_{i,j} + \tau_{j,g}\right) \cdot a_{i,j,g,v} - \tau_{k,0} \cdot \sum_{i \in N} a_{i,k,0,v} = z_v \qquad v \in V,\ k \in S. \tag{28}$$

As for the previous sets of constraints, a continuous four-dimensional variable t by the type shown in Figure 2a is defined to manage the time usage, considering 0 as the beginning time, of the vehicle when moving between nodes. In (29)–(34), the constraints on variable t were set for all nodes.

$$0 \leq t_{i,j,g,v} \leq (T_{max} \cdot a_{i,j,g,v}) \qquad v \in V,\ g \in G,\ i,j \in N, i \neq j \qquad (29)$$

$$\sum_{j \in N \setminus \{i\}} t_{j,i,g,v} - \sum_{j \in N \setminus \{i\}} t_{i,j,g,v} = \sum_{j \in \setminus \{i\}} \left[\left(h_{i,j} + \tau_{i,g} \right) \cdot a_{i,j,g,v} \right] \qquad v \in V,\ g \in G,\ i \in D \cup R \qquad (30)$$

$$t_{j,i,g,v} - (h_{j,i} \cdot a_{j,i,g,v}) = 0 \qquad v \in V,\ g = 0,\ j \in N \setminus \{i\},\ i \in S \qquad (31)$$

$$H_{i,g,v} = \sum_{k \in N \setminus \{i\}} t_{j,k,g-1,v} + \tau_{i,g} + h_{i,j} \cdot a_{i,j,g,v} \qquad v \in V,\ g \in G \setminus \{0\},\ i \in N \setminus \{j\},\ j \in S \qquad (32)$$

$$H_{i,g,v} - (1 - a_{i,j,g,v}) \cdot M \leq t_{i,j,g,v} \leq H_{i,g,v} \qquad v \in V,\ g \in G \setminus \{0\},\ i \in N \setminus \{j\},\ j \in S \qquad (33)$$

$$0 \leq t_{i,j,g,v} \leq a_{i,j,g,v} \cdot M \qquad v \in V,\ g \in G \setminus \{0\},\ i \in N \setminus \{j\},\ j \in S. \qquad (34)$$

The values in t are bounded in (29) between 0 and a maximum time allowed for service by a vehicle τ_{max}. As for (30), the time usage of the vehicle changes in the trip between nodes i and j by the time necessary for the trip plus the stop time at node i. In the beginning arc (i.e., the one leaving the depot for any other node in the first trip $g = 0$) t is equal to the time usage of that arc in (31) as the beginning time is assumed to be 0. In following trips for the same vehicle, an auxiliary variable H was defined in (32), which is used to link the time usage in the previous trip with the next one, while including the stop time at the depot. Similar to the constraints on energy management, the big-M approach was applied to variable H in (33) and (34) to maintain linearity.

A peculiarity of the developed approach is the definition of constraints related to the time intervals described by (35)–(38), which allows for linking the vehicles' trips to varying conditions within the considered time horizon.

$$\sum_{k \in T} w_{i,k,g,v} \leq \max\left(\tau_{i,g}, 1 \right) \qquad v \in V,\ g \in G,\ k \in T,\ i \in S \qquad (35)$$

$$w_{i,k,g,v} \leq 1 - [z_v - k - 0.5]/M \qquad v \in V,\ g = 0,\ k \in T,\ i \in S \qquad (36)$$

$$0.5 \cdot \tau_{i,g} \leq \sum_{j \in \setminus \{i\}} t_{i,j,g-1,v} - \sum_{k \in T} w_{i,k,g,v} \cdot (k+1) < 1 + 0.5 \cdot \tau_{i,g} \qquad v \in V,\ g \in G \setminus \{0\},\ i \in S \qquad (37)$$

$$0.5 \cdot \tau_{i,g} \leq \sum_{j \in \setminus \{i\}} t_{i,j,g,v} - \sum_{k \in T} w_{i,k,g,v} \cdot (k+1) < 1 + 0.5 \cdot \tau_{i,g} \qquad v \in V,\ g \in G,\ i \in D \cup R \qquad (38)$$

A four-dimensional binary variable w is defined by the type in Figure 2c, and it contains one in position (i, k, g, v) if vehicle v in trip g stops at node i at interval k. The sum of intervals in which any vehicle, in any trip, visits a node is constrained in (35) by the respective stop time (rounded to one hour). Although a generalization of both the interval duration and the stop time would be possible, in this work, the intervals are assumed having a one hour duration. The stop time was supposed to be less than one hour for in-service stops and multiple hours in parking mode (i.e., the period between the end of service and the beginning of a new one).

From these assumptions, in the parking period, according to (36), variable w can have multiple non-zeros, but only starting from the interval in which the last trip ends. Since, in all other occasions, the stop time is assumed to be less than one hour, constraints (37) and (38) only allow for one non-zero in those instances of variable w, which corresponds to the interval in which the vehicle is visiting the node, in the case of depot and recharging stations, respectively.

A key advantage of these constraints is that they allow the visiting time to be rounded so that it can be recorded in one or more discrete intervals in variable w to support the decisions regarding energy usage. This method lets w be non-zero in an interval when the visiting time at the node leaves more than half of the stop time in that specific hour.

A validation of the optimal outcome of the proposed methodology was conducted through comparison with other instances in the literature, as shown in Appendix A.

3. Applications and Discussion

This section reports applications of the methodology previously described to discuss how the optimal choices change according to varying energy prices, as well as due to the presence of local generation and size of the map. The maps for the instances considered in the following analysis were generated randomly to obtain hypothetical realistic cases, with the sole purpose of showing the functionality of the proposed methodology and the role of parameters on the resulting optimal decisions. It should be noted that, in practice, the location of customer nodes, charging stations, and storage facilities depend on several factors that depend not only on the land characteristics, but also on business decisions such as, for example, the type of goods delivered, the operating range, and the location of available areas.

First, a detailed analysis on a single case study is presented with multiple scenarios, where the aim is to address specific choices by the optimization methodology. Then, the outcomes of a parametric analysis are reported, considering maps with different sizes and different resource availability, to investigate the impact of those parameters on the daily cost of operation.

3.1. Specific Case Study Analysis

The case study consists of 12 overall buses dispersed in a map of 50 km length and 30 km width, with the depot being located at the top-right corner of the map, as later shown in the graphical results. Such a choice in the map size was made by considering an inter-urban type of service (i.e., a service over several customer clusters), for which the typical area was in the range of 1000–1500 km^2 [11].

Although, in practice, the stop time for service at the different nodes in the map should be computed according to the specific needs, in this study it was assumed to be 30 min for each node, according to similar works in the literature [34]. This sets the maximum duration for fast recharging during service, here assumed happening with a maximum power of 50 kW. In parking mode, slow recharge is assumed, requiring up to 6 h and with a maximum power of 7 kW. The values for maximum power in the two modes were typical for the two charging modes [57].

The EV data assumed in the following are in line with recently released commercial vehicles [58]. Average consumption is γ = 0.35 kWh/km, with an overall loading volume of 14 m^3 and a battery capacity K = 90 kWh, with $\underline{SOC}$ = 40% and $\overline{SOC}$ = 80%. Such values of SoC have been set based on studies on the suggested range of battery usage to preserve its lifetime, which should not exceed 0.2–0.8 [59]. Based on the literature about the recharging efficiency of EVs both in slow and fast charging modes, which provides a range between 85% and 90% (when considering battery chemical losses and also electrical losses in the connections and AC/DC conversion) [60,61], the recharging efficiency was considered to be equal to η_c = 90% in this study.

Vehicles were considered as traveling with an average speed σ = 50 km/h for a maximum allowed time τ_{max} = 12 h (beginning at 8 am). In the assumed context, driving time and average driving speed were assumed to be in line with the inter-urban type of service [62].

Depending on the scenario, as discussed further in this section, photovoltaic (PV) installations are supposed to be available both at the depot and at the recharging facility with a rated capacity p_g = 40 kW. A daily PV generation profile was obtained through the "PVgis" tool [63], which was achieved by considering the average daily production in the summer season in northern Italy.

In order to highlight time-dependent decisions, the energy price was assumed to vary according to the specific time interval, and it was established using time-of-use (TOU) or

real-time (RT) tariffs depending on the scenario, which were based on the prices applied in the Italian retail market for both cases. The TOU tariff adopts three time windows in a working day: T1 is from 8 a.m. to 7 p.m., T2 is from 7 a.m. to 8 a.m. and from 7 p.m. to 11 p.m., and T3 from 11 p.m. to 7 a.m. The retail price in the RT tariff, instead, was assumed to follow the trend of the energy price in the wholesale market.

The average Italian national price for the month of July 2024 was used as a reference in the simulated period. The retail price applied to energy purchases for EV recharging was obtained, both for the TOU and RT tariffs, by considering that the wholesale price only has a 50% weight (according to the average trend in the Italian retail market [64,65]). Figure 3 reports the comparison between the TOU and RT tariffs considered in the case study. In the case that PV production is available, self-consumption is priced at the wholesale energy price, as its cost corresponds to the missed revenue from selling such energy in the market.

Given the aforementioned randomly generated map, four scenarios were designed for this case study, as reported in Table 1, by combining the following options:

- Retail tariff on purchased energy, either TOU or RT, with the aforementioned assumptions;
- Presence of recharge facilities other than the depot;
- Presence of PV installation(s).

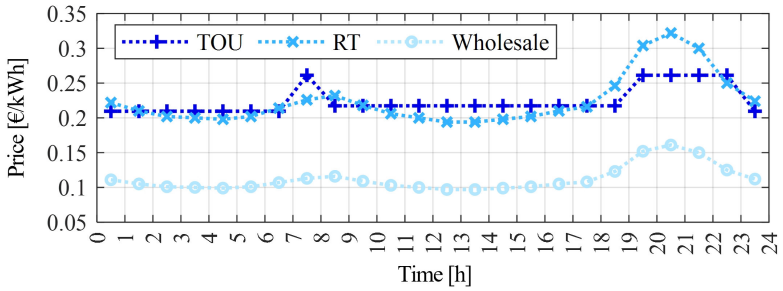

Figure 3. Time of use and real-time retail tariffs compared with the wholesale energy price.

Table 1. Setting of the conditions in the four simulated scenarios.

Scenario	Tariff	Recharging Nodes	Self Production
1	TOU	(0)	×
2	RT	(0)	×
3	RT	(0)	✓
4	RT	(0, 5)	✓

In all of the simulated scenarios, the maximum allowed operation time admitted the usage of just one vehicle. In Scenario 1, as shown in Figure 4a, the vehicle performed three trips back and forth to the depot, where the only recharging spot was located. Total time required for the service was 10.6 h (beginning at 8 a.m.). The lowest part of Figure 4a depicts the hourly intervals for service (in green) and for recharge stops at the depot node for each trip.

During the parking period, i.e., before the beginning of service and after the end of the last trip, recharging is supposed to happen at a slow rate, with a maximum power of 7 kW for up to 6 h. Through optimization, the SoC required to begin the first trip $g = 0$ was evaluated in 0.8, which translates into the purchase of 40 kWh in the low-price period T1 before beginning the first trip.

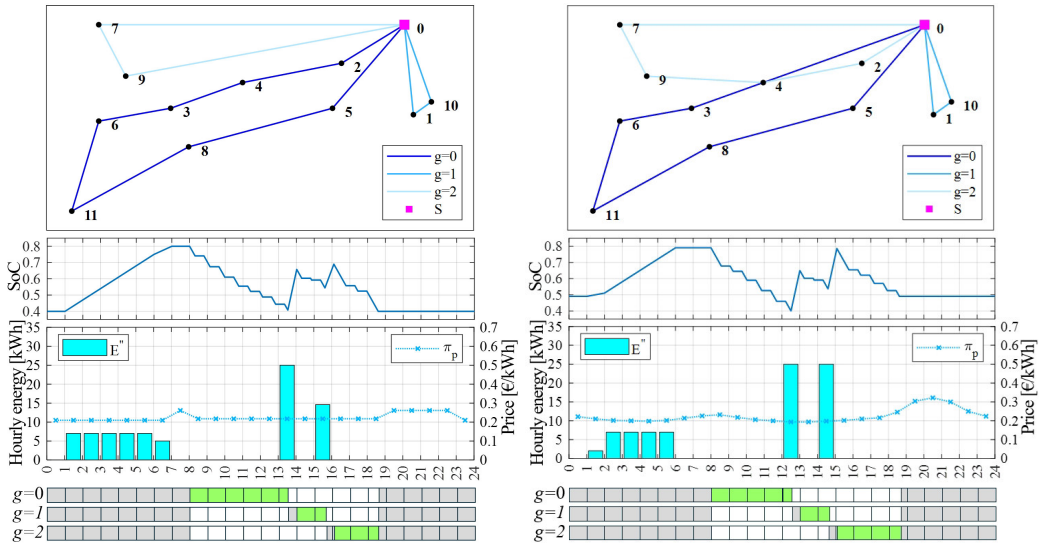

(**a**) (**b**)

Figure 4. Case study results for Scenario 1 (**a**) and Scenario 2 (**b**). The selected trips are shown in the map on top. Charts show the EV's SoC and the energy fed to the chargers compared to its price. The bottom part shows, for each trip, the traveling period (green) and the stops for recharging (gray).

During service, fast recharging was allowed with a maximum power of 50 kW, such that the 30 min stop at the depot can provide up to 25 kWh energy absorption; hence, a 22.5 kWh battery recharge. The optimal solution in Scenario 1 requires the EV to perform two intermediate stops at the depot. In the first one, occurring during Hour 14, the battery reaches the depot with SoC 0.41, and it is recharged at maximum rate, leaving the depot at SoC 0.66. A further recharge in Hour 16 was performed at the beginning of trip $g = 2$, this time only purchasing 14.6 kWh to increase the SoC from 0.54 to 0.69, which allowed for concluding service with a SoC of 0.4.

In Scenario 2, the same conditions as in Scenario 1 were considered, but the tariff on the purchased energy was the RT one. As it can be seen from the comparison on prices in Figure 3, the RT tariff has a daytime price even lower than the early morning one, with Hour 15 having the same price as Hour 5, and Hour 13 having the lowest price overall. As a result, as shown in Figure 4b, it can be seen how, compared to Scenario 1, the optimal solution led to a shorter trip $g = 0$, which was needed in order to reach the depot during Hour 13 to perform the recharging at the lowest available price. It can be noted how, in Hour 15, a further maximum fast recharge was performed, with the SoC reaching 0.79 before beginning trip $g = 2$. The service was concluded with the EV having a final SoC of 0.5, hence requiring a lower smaller purchase of 30 kWh during the parking period.

Comparing the energy usage and costs in Scenarios 1 and 2 in Table 2 it can be seen that the slight change in the route of scenario 2 requires a small increase in energy usage which grows from 79.6 kWh to 80 kWh. This reflects into a small increase in the daily energy cost from 17 € to 17.16 €.

In Scenarios 3 and 4, the presence of PV installations was considered, which allowed for exploiting self-consumption, as it can be noted from the presence of the PV production and the self-consumption trends shown in yellow and magenta, respectively, in Figure 5. In Scenario 3, although the optimal traveling route was the same as in Scenario 2, a difference in the charging pattern was found as the self-consumption was maximized. As reported in Table 2, the daily purchase of energy decreased to 43.8 kWh, which led to a cost C_{ep} of 9.39 €. The cost C_{es} amounting to 3.71 € represents the missed revenue on the 36.2 kWh of self-consumed energy.

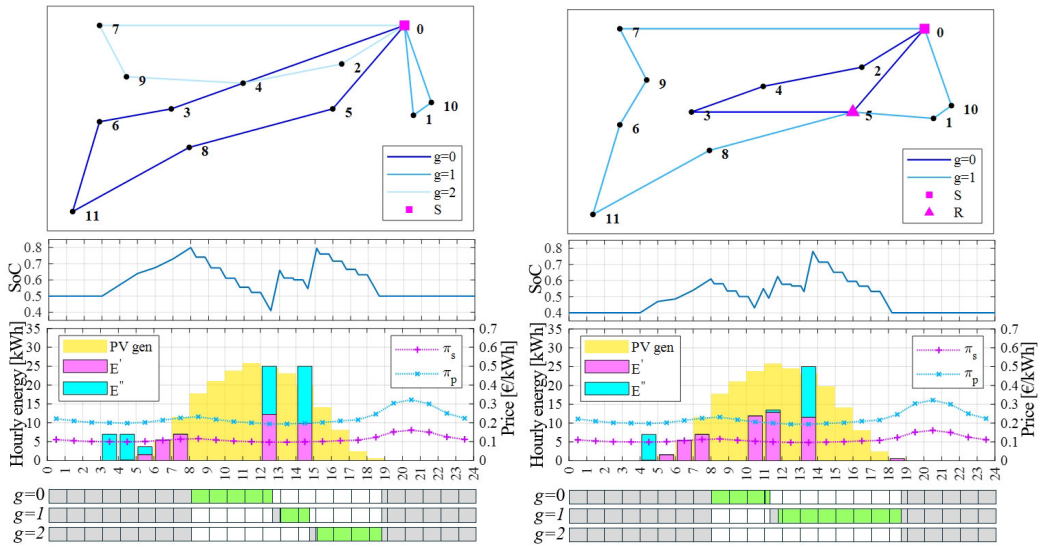

(**a**) (**b**)

Figure 5. Case study results for Scenario 3 (**a**) and Scenario 4 (**b**). The selected trips are shown in the map on top. Charts show the EV's SoC and the energy produced by PV and fed to the chargers (both self-produced and purchased) compared to the prices. The bottom part shows, for each trip, the traveling period (green) and the stops for recharging (gray).

In Scenario 4, the availability of a second recharge facility in Node 5 was considered, and it was also equipped with the same type of PV installation. The optimal route in this case changed significantly, reducing the number of trips to two. Trip g = 0 was further shortened so to allow exploiting the peak of PV production at Hour 12. The recharging facility at Node 5 was exploited both in trip g = 0 and g = 1, thus allowing to extend the EV range while maximizing the self-consumption. The purchase of energy from the grid was further reduced compared to Scenario 2, decreasing to 20.9 kWh with a daily cost of 4.49 €, while self-consumption was increased to 51.1 kWh, with missed revenues amounting to 5.25 €.

Table 2. EV energy consumption for recharging and optimal costs.

	Energy Consumption [kWh]			**Energy Cost [€]**	
	E	E'	E''	C_{es}	C_{ep}
Scenario 1	79.6	00.0	79.6	0.00	17.00
Scenario 2	80.0	00.0	80.0	0.00	17.16
Scenario 3	80.0	36.2	43.8	3.71	9.39
Scenario 4	72.0	51.1	20.9	5.25	4.49

3.2. Parametric Analysis

The results of a parametric analysis are presented in the following section, and they were achieved by considering maps with different sizes (i.e., square maps with size of 40 and 60 km, respectively). For each of the two cases, a total 100 maps were generated by randomly locating 12 nodes. Other parameters were the availability of recharging stations other than the depot and the presence of PV installations having the same characteristics assumed previously. Concerning energy pricing, the sole RT tariff was assumed for comparison purposes. The EVs in the fleet were assumed to have the same characteristics of the one investigated previously, with the only difference being the battery allowed range, which was assumed in this case to between 30% and 90% SoC.

The mean values for the main outcomes of the parametric analysis are reported in Table 3. For each case, the overall traveled distance D_{tot} and time required were reported along with the cost figures, which compose the total cost C_{tot}.

Considering the set of maps with a size of 40 km, it can be seen that the average cost for owning the vehicles was slightly higher with no recharge stations available. This fact justifies the shorter time required to complete service in such cases compared to those with at least one recharging station available. The latter ones, in fact, while requiring a longer average time to complete service, traveled a shorter distance with only one vehicle needed and a smaller overall cost. Such cost was further reduced when self-consumption was allowed by the presence of PV installations, with the minimum cost for service being found in the case with two recharge stations. The mean values reported in Table 3 show that the traveling distance increased by 2% in these cases, which allowed for maximizing the self-consumption, thus leading to a total cost decrease in the range of 6–11%.

Table 3. Mean of the main outcomes of the parametric analysis. Simulated cases are defined by Size: length of each map side; PV: availability of PV generation, yes (✓) or no (×); and #R: the number of recharging facilities.

Size	PV	#R	D_{tot} [km]	*Time* [h]	C_v [€]	C_{es} [€]	C_{ep} [€]	C_{tot} [€]
40	×	0	149.27	8.58	22.00	0.00	12.86	34.86
40	×	1	147.75	8.97	20.00	0.00	12.52	32.52
40	×	2	147.68	8.96	20.00	0.00	12.40	32.40
40	✓	0	152.94	8.71	22.40	3.51	6.94	32.84
40	✓	1	150.00	9.21	20.00	3.90	5.81	29.70
40	✓	2	150.41	9.18	20.20	5.11	3.61	28.92
60	×	0	247.25	7.54	38.82	0.00	21.25	60.07
60	×	1	225.99	8.13	34.40	0.00	19.44	53.84
60	×	2	214.88	8.45	33.60	0.00	18.39	51.99
60	✓	0	263.41	7.07	40.00	8.17	7.63	55.80
60	✓	1	245.47	7.64	34.75	7.40	7.59	49.74
60	✓	2	244.19	7.77	34.11	7.84	6.54	48.48

Considering now the set of bigger maps with sizes of 60 km, it can be seen how, although the trend on energy costs was confirmed, a higher variability on the EV ownership cost was found, with more cases requiring the usage of two EVs. This was evident especially when comparing cases without and with the availability of self-production, with the latter resulting in a shorter traveling time, thus indicating the use of more vehicles on average. Overall, the cost reduction from self-consumption was confirmed to in the range of 7–8%.

The distribution of C_{tot} values in the simulated instances is reported in Figure 6, which shows the ranges between the 1–99, 10–90, and 25–75 percentiles along with the mean value. It can be noted how, for smaller maps, the presence of at least one recharging station, other than the depot, led to more homogeneous, and lower, costs. In the case of bigger maps, a wider distribution of total cost was found due to a higher variability in the chosen paths, especially in the cases with available recharging stations. It can be seen that, although the mean cost reduction was in line with the trend observed in smaller maps, when comparing the range of results between the 25th and 75th percentiles, the costs can become significantly lower when considering recharging stations as they allow one to exploit the time variation of prices.

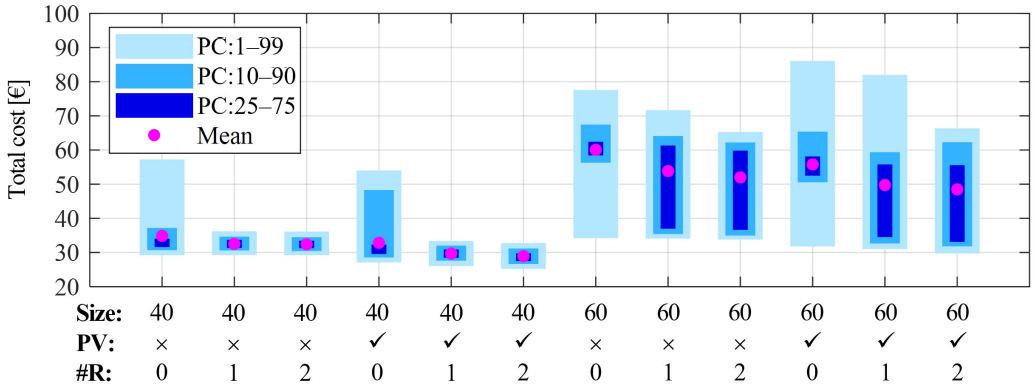

Figure 6. Distribution of costs in the parametric analysis, for each case given by the combination of: length of each map side in km (Size), availability of PV generation (PV): yes (✓) or no (×), and number of recharging facilities (#R). The mean value and percentile ranges are shown.

4. Conclusions

Despite substantial evidence that the use of electric vehicles (EVs) in logistics offers numerous advantages, including reducing greenhouse gas (GhG) emissions (thanks to the use of more renewable energies as energy sources), improving urban traffic management, and potentially supporting the electric power system via vehicle-to-grid (V2G) technology, their adoption in this sector remains limited. Key barriers include battery range limitations, charging time, and the availability of recharging infrastructure. Addressing these challenges requires strategic planning and optimization to maximize the benefits of EVs while mitigating operational constraints.

This paper introduces a comprehensive methodology for optimally planning freight distribution services when using EVs in a generic map of delivery nodes. The methodology accounts for recharging opportunities both at depots and en route, enabling a more flexible and efficient operation of EV fleets. It focuses on a single layer within a multi-tier freight distribution scheme, aiming to generalize the approach to plan EV fleet size and organize vehicle trips based on parameters that vary across both spatial and temporal dimensions.

A distinctive feature of the proposed approach is its use of multi-period optimization. This framework incorporates local energy production profiles and time-dependent energy purchase prices to strategically schedule charging operations over a defined planning horizon. By aligning charging activities with energy cost fluctuations and availability, the methodology enhances the cost-effectiveness and sustainability of EV logistics. This is also compliant with the necessity to increase the integration of renewable energy sources in the distribution network: in this sense, the promotion of this kind of systems is also strategic from a policy perspective.

Simulation results on various case studies illustrate the critical role of resource availability—such as charging facilities and energy self-production—as they are distributed across space and time, as well as due to their interaction with dynamic electricity tariffs. A parametric analysis on a set of randomly generated maps revealed significant cost reductions, which were achieved by incorporating multiple recharging facilities into the planning scheme. These benefits were particularly pronounced for larger geographic areas, where the methodology identified more differentiated solutions, leading to greater overall cost savings.

The primary focus of this study was not on computational efficiency but on establishing a robust foundational framework for optimization. Future research will explore alternative heuristic solutions derived from the current setup, with the aim of improving computational scalability. Additionally, the methodology presented in this paper opens up avenues for exploring public–private partnership (PPP) schemes. By designing tariffs tailored to both the spatial and temporal characteristics of electricity usage, these schemes could influence

urban traffic patterns and the operation of the electric distribution grid, thereby enhancing the integration of EVs into urban infrastructure. This aspect shall be deeply discussed with local authorities, who need specialized competences to support their decisions in the field.

Further research could extend this work by applying a similar comparative modeling approach to other types of vehicles, such as buses powered by diesel or gas engines. In this case, we will need to analyze the integration among different energy sources, keeping the option of electrification as a policy priority (when possible). Such studies would provide valuable insights into the broader applicability of the proposed methodologies across various transport sectors.

Author Contributions: Conceptualization, M.C., M.A. and G.D.M.; methodology, M.C. and M.A.; investigation, M.C., M.A. and G.D.M.; resources, M.C., G.D.M. and M.B.; writing—original draft preparation, M.C., G.D.M. and M.B.; writing—review and editing, M.C. and M.B.; supervision, M.C. and M.B. All authors have read and agreed to the published version of the manuscript.

Funding: "GRINS—Growing Resilient, INclusive and Sustainable" Partenariato Esteso Tematica 9 "Economic and financial sustainability of systems and territories" Piano Nazionale di Ripresa e Resilienza MUR PE00000018—CUP C93C22005270001, Missione 4 "Istruzione e ricerca"—Componente 2 "Dalla ricerca all'impresa"–Investimento 1.3, finanziato dall'Unione europea—NextGenerationEU"—Spoke 6.

Data Availability Statement: The original contributions presented in this study are included in the article, further inquiries can be directed to the corresponding authors.

Acknowledgments: Marina Bertolini and Massimiliano Coppo acknowledge the Interdepartmental Centre for Energy Economics and Technology "Giorgio Levi Cases", Padova, Italy, for its support under project INCITE.

Conflicts of Interest: The authors declare no conflicts of interest.

Nomenclature and Acronyms

The following acronyms, sets, parameters, and variables are used in the manuscript:

Acronym	**Description**
CO_2	Carbon Dioxide
GhG	Greenhouse Gases
EV	Electric Vehicle
EU	European Union
TCO	Total Cost of Ownership
BEV	Battery Electric Vehicle
FCV	Fuel Cell Vehicle
IECV	Internal Combustion Engine Vehicle
PPP	Public–Private Partnership
EVRP	Electric Vehicle Routing Problem
V2G	Vehicle-To-Grid
MILP	Mixed Integer Linear Programming
SoC	State of Charge
TOU	Time Of Use
RT	Real Time
PV	Photovoltaic
Set	**Description**
N	Set of all map nodes
D	Set of delivery nodes
S	Set of depots
G	Set of trips
V	Set of vehicles

R	Set of delivery nodes with recharging facility
T	Set of all time intervals
Parameter	**Description**
c_{ev}	Cost for the availability of a vehicle during the time horizon [€]
x_i, y_i	Coordinates of node i [km]
$d_{i,j}$	Distance in arc $i-j$ [km]
$b_{i,j}$	Energy required by arc $i-j$ [kWh]
$h_{i,j}$	Time required by arc $i-j$ [h]
$\pi_{s,i,k}$	Price applied to self-produced energy [€/kWh]
$\pi_{p,i,k}$	Price applied to purchased energy [€/kWh]
p_g	Generated power in each time interval (average) [kW]
p_r	Allowed recharge power in node and trip [kW]
q_i	Freight quantity required at node i [m^3]
τ	Stop for node and trip [h]
τ_{max}	Stop for node and trip [h]
γ_v	Energy consumption by vehicle v [kWh/km]
$sigma_v$	Average driving speed of vehicle v [km/h]
cap_v	Freight capacity of vehicle v [m^3]
K_v	Battery capacity in vehicle v [kWh]
$\overline{SOC}_v$	Maximum State Of Charge of vehicle v
$\underline{SOC}_v$	Minimum State Of Charge of vehicle v
η_c	Charging efficiency
M	Large arbitrary number
Variable	**Description**
C_v	Cost for fleet availability [€]
C_{es}	Missed revenue from self-production sale [€]
C_{ep}	Cost for purchasing energy [€]
a	Enabled arcs
w	Active time window for recharging
f	Freight volume in vehicle, in arc [m^3]
e	Energy in vehicle's battery in arc [kWh]
t	Cumulated time in arc [h]
z	Total travel time by each vehicle [h]
E	Energy absorption [kWh]
E'	Self-produced energy [kWh]
E''	Purchased energy [kWh]
J, H	Support variables for *big-M* method

Appendix A

For the sake of validating the results obtained with the proposed methodology, a comparison with results taken from the literature is reported in this section. In particular, the problems considered in the following comparison were used to propose an electric vehicle routing problem with multiple recharging technologies in [44]. From the repository related to the mentioned work [66], Dataset A was used, which consists of vehicle routing problems derived from previously published works which were adapted to include the possibility of recharging electric vehicles with homogeneous technology. The 36 instances in Dataset A include sets with a number of customers (C) up to 15 and a number of recharging stations (#R) up to 7. For each instance, the coordinates of each node was reported, along with the energy consumption and time required in each arc, and these were used to create sets d, b, and h, respectively. For each node, a request in terms of freight and time was declared, hence defining sets q and τ. The number of available vehicles was provided, along with the total time τ_{max} allowed for service and technical data such as the available battery capacity K and freight capacity cap.

In order to use the same conditions considered in [66], the simulations were performed with the following settings. As the indicated battery capacity represents the available range, $\underline{SOC}$ and $\overline{SOC}$ were assumed to be 0 and 1, respectively, while η_c was set to 1 in absence of other information. The published study assumed each route pertaining to a different vehicle in a given fleet size; therefore, no cost was considered for the fleet increase, i.e., $c_{ev} = 0$, while each vehicle had only one trip available, i.e., $G = \{0\}$. Since the time varying price of energy was not considered, a constant unitary price had been assumed, such that the resulting total cost C_{tot} in [€] was equivalent to the amount of purchased energy. No self production was assumed; therefore, all the recharging energy was purchased from the grid.

Finally, the solution to instances in the dataset considered the possibility, for a vehicle, to return to a recharging station during the same trip and to not visit a recharging station node, which was not allowed with the proposed methodology detailed in Section 2; therefore, some expedients had to be used to comply with the published results. The recharging stations buses were doubled, creating additional recharging stations in the same location of the original ones, hence allowing for a further visit. To include the option of not visiting nodes hosting charging stations, constraints (10) and (11) were modified by changing the inequality sign to $\leq$.

Results of the comparison between the solutions in [66] and the simulations are reported in Table A1. The referenced results include the number of routes and the total cost for energy purchase, while the simulation results also report the total distance traveled (for contextualization). Finally, the relative percent variation (Δ) between the reference and simulation is reported in the last column of Table A1.

As it can be seen, in 28 out of 36 cases, the results obtained using the methodology described in Section 2 provided the same exact results as in [66]. In 8 of the cases, the solution found provided an even smaller cost, with a relative percent variation of up to -10.56%, indicating a shorter traveled distance. Among these, in 6 of the instances, the simulation evaluated a solution with a smaller number of routes, namely C101-10, C104-10, R104-5, R105-15, R105-5, and RC205-10.

Table A1. Comparison of the results from the proposed algorithm and reference [66].

			Reference		**Simulation**			
Instance	**C**	**#R**	**Routes**	C_{tot}	**Routes**	C_{tot}	D_{tot}	**Δ**
C101-5	5	2	1	214	1	214	208.9	0.00%
C103-5	5	1	1	157	1	157	154.5	0.00%
C206-5	5	3	1	205	1	205	201.5	0.00%
C208-5	5	2	1	161	1	161	158.5	0.00%
R104-5	5	2	2	142	1	142	137.8	0.00%
R105-5	5	2	2	160	1	160	156.1	0.00%
R202-5	5	2	1	147	1	147	143.4	0.00%
R203-5	5	3	1	185	1	185	179.1	0.00%
RC105-5	5	3	2	220	2	220	214.6	0.00%
RC108-5	5	3	2	259	2	259	253.9	0.00%
RC204-5	5	3	1	182	1	182	176.4	0.00%
RC208-5	5	2	1	172	1	172	168.0	0.00%

Table A1. *Cont.*

			Reference		Simulation			
Instance	**C**	**#R**	**Routes**	C_{tot}	**Routes**	C_{tot}	D_{tot}	**Δ**
C101-10	10	4	2	303	1	271	263.1	−10.56%
C104-10	10	3	2	281	1	259	252.1	−7.83%
C202-10	10	4	1	234	1	234	223.7	0.00%
C205-10	10	2	2	233	2	233	227.1	0.00%
R102-10	10	3	2	230	2	230	221.0	0.00%
R103-10	10	2	2	169	2	169	160.4	0.00%
R201-10	10	3	1	189	1	189	183.1	0.00%
R203-10	10	4	1	252	1	252	243.1	0.00%
RC102-10	10	3	3	428	3	410	403.1	−4.21%
RC108-10	10	3	3	355	3	355	345.5	0.00%
RC201-10	10	3	1	258	1	258	249.1	0.00%
RC205-10	10	3	2	320	1	320	311.7	0.00%
C103-15	15	4	2	290	2	290	280.2	0.00%
C106-15	15	2	2	253	2	237	226.8	−6.32%
C202-15	15	4	1	332	1	332	320.4	0.00%
C208-15	15	3	1	269	2	269	262.5	0.00%
R102-15	15	7	3	317	3	305	293.2	−3.79%
R105-15	15	5	3	297	2	293	284.4	−1.35%
R202-15	15	5	1	286	1	286	275.0	0.00%
R209-15	15	4	1	264	1	264	257.1	0.00%
RC103-15	15	4	3	367	3	356	345.1	−3.00%
RC108-15	15	4	3	384	3	359	345.8	−6.51%
RC202-15	15	4	1	305	1	305	295.6	0.00%
RC204-15	15	6	1	295	1	295	285.4	0.00%

References

1. IEA. Global CO_2 Emissions from Transport by Subsector, 2000–2030. 2021. Available online: https://www.iea.org/data-and-statistics/charts/global-co2-emissions-from-transport-by-subsector-2000-2030 (accessed on 3 September 2024).
2. IEA. World Energy Outlook 2024. 2024. Available online: https://www.iea.org/reports/world-energy-outlook-2024 (accessed on 3 September 2024).
3. European Parliament, Council of the European Union. Regulation (EU) 2019/631 of the European Parliament and of the Council of 17 April 2019 Setting CO_2 Emission Performance Standards for New Passenger Cars and for New Light Commercial Vehicles, and Repealing Regulations (EC) No 443/2009 and (EU) No 510/2011. 2019. Available online: http://data.europa.eu/eli/reg/2019/631/oj (accessed on 4 November 2024).
4. Milojević, S.; Glišović, J.; Savić, S.; Bošković, G.; Bukvić, M.; Stojanović, B. Emissioni di particolato e riduzione dell'inquinamento atmosferico mediante l'applicazione di sistemi variabili in motori diesel tribologicamente ottimizzati per veicoli nel traffico stradale. *Atmosphere* **2024**, *15*, 184. [CrossRef]
5. European Parliament, Council of the European Union. Directive (EU) 2018/2001 of the European Parliament and of the Council of 11 December 2018 on the Promotion of the Use of Energy from Renewable Sources. 2018. Available online: http://data.europa.eu/eli/dir/2018/2001/oj (accessed on 4 November 2024).
6. IEA. Global EV Outlook 2022: Securing Supplies for an Electric Future. 2022. Available online: https://www.oecd.org/en/publications/global-ev-outlook-2022_c83f815c-en.html (accessed on 3 September 2024).
7. Tsoi, K.H.; Loo, B.P.Y. A people-environment framework in evaluating transport stress among rail commuters. *Transp. Res. Part Transp. Environ.* **2023**, *121*, 103833. [CrossRef]
8. Mommens, K.; Lebeau, P.; Verlinde, S.; van Lier, T.; Macharis, C. Evaluating the impact of off-hour deliveries: An application of the TRansport Agent-BAsed model. *Transp. Res. Part Transp. Environ.* **2018**, *62*, 102–111. [CrossRef]
9. Lu, F.; Du, Z.; Wang, Z.; Wang, L.; Wang, S. Towards enhancing the crowdsourcing door-to-door delivery: An effective model in Beijing. *J. Ind. Manag. Optim.* **2025**, *21*, 2371–2395. [CrossRef]
10. Alarcón, F.E.; Mac Cawley, A.; Sauma, E. Electric mobility toward sustainable cities and road-freight logistics: A systematic review and future research directions. *J. Clean. Prod.* **2023**, *430*, 138959. [CrossRef]

11. Morganti, E.; Browne, M. Technical and operational obstacles to the adoption of electric vans in France and the UK: An operator perspective. *Transp. Policy* **2018**, *63*, 90–97. [CrossRef]
12. Axsen, J.; Pickrell-Barr, J. What drives fleets? Organizations' perceived barriers and motivators for alternative-fuel vehicles. *Transp. Res. Part Transp. Environ.* **2024**, *132*, 104220. [CrossRef]
13. Figenbaum, E. Can battery electric light commercial vehicles work for craftsmen and service enterprises? *Energy Policy* **2018**, *120*, 58–72. [CrossRef]
14. Quak, H.; Nesterova, N.; van Rooijen, T. Possibilities and barriers for using electric-powered vehicles in city logistics practice. *Transp. Res. Procedia* **2016**, *12*, 157–169. [CrossRef]
15. Juan, A.A.; Mendez, C.A.; Faulin, J.; De Armas, J.; Grasman, S.E. Electric vehicles in logistics and transportation: A survey on emerging environmental, strategic, and operational challenges. *Energies* **2016**, *9*, 86. [CrossRef]
16. Wijngaarden, L.; Schroten, A.; Essen, H.; Sutter, D.; Andrew, E. *Sustainable Transport Infrastructure Charging and Internalisation of Transport Externalities—Executive Summary*; European Commission and Directorate-General for Mobility and Transport: Delft, The Netherlands, 2019. [CrossRef]
17. Brent, D.; Beland, L.P. Traffic congestion, transportation policies, and the performance of first responders. *J. Environ. Econ. Manag.* **2020**, *103*, 102339. [CrossRef]
18. European Commission. Communication from the Commission to the European Parliament, the Council, the European Economic and Social Committee and the Committee of the regions—Sustainable and Smart Mobility Strategy—Putting European Transport on Track for the Future. 2020. Available online: https://eur-lex.europa.eu/legal-content/EN/TXT/?uri=CELEX:52020DC0789 (accessed on 23 October 2024).
19. Russo, F.; Comi, A. Investigating the Effects of City Logistics Measures on the Economy of the City. *Sustainability* **2020**, *12*, 1439. [CrossRef]
20. Wijnen, W.; Stipdonk, H. Social costs of road crashes: An international analysis. *Accid. Anal. Prev.* **2016**, *94*, 97–106. [CrossRef]
21. Schoeters, A.; Large, M.; Koning, M.; Carnis, L.; Daniels, S.; Mignot, D.; Urmeew, R.; Wijnen, W.; Bijleveld, F.; van der Horst, M. Economic valuation of preventing fatal and serious road injuries. Results of a Willingness-To-Pay study in four European countries. *Accid. Anal. Prev.* **2022**, *173*, 106705. [CrossRef] [PubMed]
22. Atlas Public Policy. *Assessing Financial Barriers to the Adoption of Electric Trucks*; Technical Report; Atlas Public Policy: Washington, DC, USA, 2020.
23. Satterfield, C.; Nigro, N. *A Total Cost of Ownership Analysis*; *International Council on Clean Transportation*: Washington, DC, USA, 2023.
24. Song, Y.; Shangguan, L.; Li, G. Simulation analysis of flexible concession period contracts in electric vehicle charging infrastructure public-private-partnership (EVCI-PPP) projects based on time-of-use (TOU) charging price strategy. *Energy* **2021**, *228*, 120328. [CrossRef]
25. Alnour, M.; Awan, A.; Hossain, M.E. Towards a green transportation system in Mexico: The role of renewable energy and transport public-private partnership to curb emissions. *J. Clean. Prod.* **2024**, *442*, 140984. [CrossRef]
26. Bertolini, M.; De Matteis, G.; Nava, A. Sustainable Last-Mile Logistics in Economics Studies: A Systematic Literature Review. *Sustainability* **2024**, *16*, 1205. [CrossRef]
27. Holman, C.; Harrison, R.; Querol, X. Review of the efficacy of low emission zones to improve urban air quality in European cities. *Atmos. Environ.* **2015**, *111*, 161–169. [CrossRef]
28. Ellison, R.B.; Greaves, S.P.; Hensher, D.A. Five years of London's low emission zone: Effects on vehicle fleet composition and air quality. *Transp. Res. Part Transp. Environ.* **2013**, *23*, 25–33. [CrossRef]
29. Fu, J.; Jenelius, E. Transport efficiency of off-peak urban goods deliveries: A Stockholm pilot study. *Case Stud. Transp. Policy* **2018**, *6*, 156–166. [CrossRef]
30. Hriekova, O.; Galkin, A.; Schlosser, T.; Prasolenko, O.; Sokolova, N. Planning of Urban Freight Delivery During Peak and Off-Peak Traffic Periods. In Proceedings of the Internet of Everything, Guimarães, Portugal, 28–29 September 2023; Pereira, T., Impagliazzo, J., Santos, H., Chen, J., Eds.; Springer: Cham, Switzerland, 2024; pp. 126–138. [CrossRef]
31. Marcucci, E.; Gatta, V.; Scaccia, L. Urban freight, parking and pricing policies: An evaluation from a transport providers' perspective. *Transp. Res. Part Policy Pract.* **2015**, *74*, 239–249. [CrossRef]
32. de Palma, A.; Lindsey, R. Traffic congestion pricing methodologies and technologies. *Transp. Res. Part Emerg. Technol.* **2011**, *19*, 1377–1399. [CrossRef]
33. Holguín-Veras, J.; Sánchez-Díaz, I. Freight Demand Management and the Potential of Receiver-Led Consolidation programs. *Transp. Res. Part Policy Pract.* **2016**, *84*, 109–130. [CrossRef]
34. Anderluh, A.; Hemmelmayr, V.C.; Nolz, P.C. Synchronizing vans and cargo bikes in a city distribution network. *Cent. Eur. J. Oper. Res.* **2017**, *25*, 345–376. [CrossRef]

35. Enthoven, D.L.J.U.; Jargalsaikhan, B.; Roodbergen, K.J.; uit het Broek, M.A.J.; Schrotenboer, A.H. The two-echelon vehicle routing problem with covering options: City logistics with cargo bikes and parcel lockers. *Comput. Oper. Res.* **2020**, *118*, 104919. [CrossRef]
36. Marcucci, E.; Le Pira, M.; Gatta, V.; Inturri, G.; Ignaccolo, M.; Pluchino, A. Simulating participatory urban freight transport policy-making: Accounting for heterogeneous stakeholders' preferences and interaction effects. *Transp. Res. Part Logist. Transp. Rev.* **2017**, *103*, 69–86. [CrossRef]
37. Elbert, R.; Rentschler, J. Freight on urban public transportation: A systematic literature review. *Res. Transp. Bus. Manag.* **2022**, *45*, 100679. [CrossRef]
38. Delle Donne, D.; Alfandari, L.; Archetti, C.; Ljubić, I. Freight-on-Transit for urban last-mile deliveries: A strategic planning approach. *Transp. Res. Part Methodol.* **2023**, *169*, 53–81. [CrossRef]
39. Kucukoglu, I.; Dewil, R.; Cattrysse, D. The electric vehicle routing problem and its variations: A literature review. *Comput. Ind. Eng.* **2021**, *161*, 107650. [CrossRef]
40. Cattaruzza, D.; Absi, N.; Feillet, D.; González-Feliu, J. Vehicle routing problems for city logistics. *Euro J. Transp. Logist.* **2017**, *6*, 51–79. [CrossRef]
41. Verma, A. Electric vehicle routing problem with time windows, recharging stations and battery swapping stations. *Euro J. Transp. Logist.* **2018**, *7*, 415–451. [CrossRef]
42. Montoya, A.; Guéret, C.; Mendoza, J.E.; Villegas, J.G. The electric vehicle routing problem with nonlinear charging function. *Transp. Res. Part Methodol.* **2017**, *103*, 87–110. [CrossRef]
43. Ceselli, A.; Felipe, Á.; Ortuño, M.T.; Righini, G.; Tirado, G. A branch-and-cut-and-price algorithm for the electric vehicle routing problem with multiple technologies. *Oper. Res. Forum* **2021**, *2*, 8. [CrossRef]
44. Bezzi, D.; Ceselli, A.; Righini, G. A route-based algorithm for the electric vehicle routing problem with multiple technologies. *Transp. Res. Part Emerg. Technol.* **2023**, *157*, 104374. [CrossRef]
45. Lin, B.; Ghaddar, B.; Nathwani, J. Electric vehicle routing with charging/discharging under time-variant electricity prices. *Transp. Res. Part Emerg. Technol.* **2021**, *130*, 103285. [CrossRef]
46. He, J.; Yan, N.; Zhang, J.; Yu, Y.; Wang, T. Battery electric buses charging schedule optimization considering time-of-use electricity price. *J. Intell. Connect. Veh.* **2022**, *5*, 138–145. [CrossRef]
47. Noori, M.; Zhao, Y.; Onat, N.C.; Gardner, S.; Tatari, O. Light-duty electric vehicles to improve the integrity of the electricity grid through Vehicle-to-Grid technology: Analysis of regional net revenue and emissions savings. *Appl. Energy* **2016**, *168*, 146–158. [CrossRef]
48. Quddus, M.A.; Kabli, M.; Marufuzzaman, M. Modeling electric vehicle charging station expansion with an integration of renewable energy and Vehicle-to-Grid sources. *Transp. Res. Part Logist. Transp. Rev.* **2019**, *128*, 251–279. [CrossRef]
49. Raveendran, V.; Alvarez-Bel, C.; Nair, M.G. Assessing the ancillary service potential of electric vehicles to support renewable energy integration in touristic islands: A case study from Balearic island of Menorca. *Renew. Energy* **2020**, *161*, 495–509. [CrossRef]
50. Agostini, M.; Bertolini, M.; Coppo, M.; Fontini, F. The participation of small-scale variable distributed renewable energy sources to the balancing services market. *Energy Econ.* **2021**, *97*, 105208. [CrossRef]
51. Coppo, M.; Bignucolo, F.; Turri, R. Sliding time windows assessment of storage systems capability for providing ancillary services to transmission and distribution grids. *Sustain. Energy, Grids Netw.* **2021**, *26*, 100467. [CrossRef]
52. Engelhardt, J.; Grillo, S.; Calearo, L.; Agostini, M.; Coppo, M.; Marinelli, M. Optimal control of a DC microgrid with busbar matrix for high power EV charging. *Electr. Power Syst. Res.* **2023**, *224*, 109680. [CrossRef]
53. Bignucolo, F.; Mantese, L. Controllable Meshing of Distribution Grids through a Multi-Leg Smart Charging Infrastructure (MLSCI). *Energies* **2024**, *17*, 1960. [CrossRef]
54. De Cauwer, C.; Van Mierlo, J.; Coosemans, T. Energy consumption prediction for electric vehicles based on real-world data. *Energies* **2015**, *8*, 8573–8593. [CrossRef]
55. Bi, J.; Wang, Y.; Sai, Q.; Ding, C. Estimating remaining driving range of battery electric vehicles based on real-world data: A case study of Beijing, China. *Energy* **2019**, *169*, 833–843. [CrossRef]
56. Shabanzadeh, M.; Sheikh-El-Eslami, M.K.; Haghifam, M.R. Risk-based medium-term trading strategy for a virtual power plant with first-order stochastic dominance constraints. *IET Gener. Transm. Distrib.* **2017**, *11*, 520–529. [CrossRef]
57. Shareef, H.; Islam, M.M.; Mohamed, A. A review of the stage-of-the-art charging technologies, placement methodologies, and impacts of electric vehicles. *Renew. Sustain. Energy Rev.* **2016**, *64*, 403–420. [CrossRef]
58. Mercedes-Benz. The New eSprinter Large Electric Panel Van. Available online: https://www.mercedes-benz.co.uk/vans/models/esprinter/panel-van/overview.html (accessed on 6 November 2024).
59. Woody, M.; Arbabzadeh, M.; Lewis, G.M.; Keoleian, G.A.; Stefanopoulou, A. Strategies to limit degradation and maximize Li-ion battery service lifetime-Critical review and guidance for stakeholders. *J. Energy Storage* **2020**, *28*, 101231. [CrossRef]
60. Apostolaki-Iosifidou, E.; Codani, P.; Kempton, W. Measurement of power loss during electric vehicle charging and discharging. *Energy* **2017**, *127*, 730–742. [CrossRef]

61. Gjelaj, M.; Træholt, C.; Hashemi, S.; Andersen, P.B. Optimal design of DC fast-charging stations for EVs in low voltage grids. In Proceedings of the 2017 IEEE Transportation Electrification Conference and Expo (ITEC), Chicago, IL, USA, 22–24 June 2017; pp. 684–689.
62. European Commission, Directorate-General for Mobility and Transport. Ex-Post Evaluation of Directive 92/6/EEC on the Installation and Use of Speed Limitation Devices for Certain Categories of Motor Vehicles in the Community, as Amended by Directive 2002/85/EC. 2013. Available online: https://op.europa.eu/en/publication-detail/-/publication/6741cad5-38ce-4102-8887-14bebbafc81b (accessed on 3 January 2025).
63. European Commission, Joint Research Centre (JRC). Photovoltaic Geographical Information System—PVGIS. Available online: https://re.jrc.ec.europa.eu/pvg_tools/en/ (accessed on 23 October 2024).
64. Gestore Mercati Energetici—GME. Average Price by Band. Available online: https://www.mercatoelettrico.org/en-us/Home/Publications/AveragePriceBand (accessed on 23 October 2024).
65. ARERA. Annual Report on the State of Services and Regulatory Activities Carried Out During 2023. Available online: https://www.arera.it/en/publications/annual-report (accessed on 23 October 2024).
66. Bezzi, D. Electric Vehicle Routing Problem with Multiple Recharge Technologies (EVRP-MRT) Dataset. 2021. Available online: https://doi.org/10.13130/RD_UNIMI/JEA5XX (accessed on 30 December 2024).